

# Bound of Casimir Effect by Holography

Rong-Xin Miao

*School of Physics and Astronomy, Sun Yat-Sen University, Zhuhai, 519082, China*

Inspired by the Kovtun-Son-Starinet bound, we propose that holography impose a lower bound on the Casimir effect. For simplicity, we focus on the Casimir effect between parallel planes for 3d conformal field theories and briefly comment on the generalizations to other boundary shapes and higher dimensions. Remarkably, the ghost-free holographic models impose a universal lower bound of the Casimir effect. We verify the holographic bound by free theories, Ising model, and  $O(N)$  model with  $N = 2, 3$  at critical points. Remarkably, the holographic bound is also obeyed by a general class of quantum field theories without conformal symmetries. It is interesting to find a field-theoretical proof or counterexample for the holographic bound of Casimir effect.

*Introduction* — Casimir effect [1] is a novel quantum effect that originates from the changes of vacuum fluctuations due to the boundary [2–5]. It is a candidate of dark energy [6] and plays a vital role in QCD [7] and wormhole physics [8, 9]. It has been measured in experiments [10–12] and has significant potential applications in nanotechnology. As the vacuum energy, Casimir energy is defined as the lowest energy of a quantum system with a boundary. Since energy should be bounded from the below, it is expected that there is a fundamental lower bound of the Casimir effect. This paper explores this vital problem. Holography (AdS/CFT) [13] provides a powerful tool to study the strongly coupled conformal field theory (CFT) and usually imposes bounds on various physical phenomena. The most famous example is the Kovtun-Son-Starinet (KSS) bound [14] for hydrodynamics, which conjectures that the ratio of shear viscosity  $\eta$  and entropy density  $s$  has a lower bound

$$\frac{\eta}{s} \geq \frac{\hbar}{4\pi k_B}, \quad (1)$$

where  $\hbar$  is the reduced Planck constant and  $k_B$  is the Boltzmann constant. The lower bound is obtained from the strongly-coupled CFT dual to Einstein gravity [15] and can be modified slightly by higher derivative gravity [16–18].

Now, let us explore whether AdS/CFT set a similar lower bound for the Casimir effect. For simplicity, we focus on the Casimir effect for 3d CFTs between parallel planes (strip) and comment on various generalizations at the end of the paper. We consider flat space and impose the same boundary conditions on the two planes. Then, the Casimir effect takes a universal form

$$\langle T_{\bar{j}}^i \rangle_{\text{strip}} = \kappa_1 \frac{\hbar c}{L^3} \text{diag}\left(1, -2, 1\right), \quad (2)$$

where  $\kappa_1$  is the dimensionless Casimir amplitude,  $c$  is the speed of light,  $L$  is the distance between the two plates. For a CFT with fixed strip width  $L$ ,  $(-\kappa_1)$  should be bounded from below to avoid negative infinity energy density ( $T_{tt} = -\kappa_1 \hbar c / L^3$ ) and pressure ( $T_{nn} = -2\kappa_1 \hbar c / L^3$ ). Note that the Casimir amplitude  $\kappa_1$  is an extensive parameter in the sense that if one CFT

has a Casimir amplitude  $\kappa_1$ , then  $N$ -copies of the same CFT has a Casimir amplitude  $N\kappa_1$ . It implies only  $(-\kappa_1)$  over another extensive parameter could have a lower bound. Natural candidates of these extensive parameters are the central charges of CFTs. Since the Casimir effect is a boundary effect, the most natural candidates are boundary central charges defined in Weyl anomaly[19]  $\mathcal{A} = \int_{\partial M} d^2x \sqrt{|\sigma|} \left( a R_{\partial M} + b \text{tr} \bar{k}^2 \right)$ , where  $R_{\partial M}$  and  $\bar{k}$  are the intrinsic Ricci scalar and traceless parts of extrinsic curvatures on the boundary  $\partial M$ , respectively.  $a$  is the A-type boundary central charge, which decreases under the boundary RG flow [19]. We remark that  $a$  can be positive, zero, or negative. For example,  $a = \pm 1/(384\pi)$  for conformally coupled free scalar with Robin boundary condition (RBC) and Dirichlet boundary condition (DBC) [19], respectively;  $a \sim \sinh(\rho)$  with  $-\infty < \rho < \infty$  for holographic CFT<sub>3</sub> [20]. Since  $a$  can be zero and negative, there is no lower bound for  $(-\kappa_1/a)$ . On the other hand, the B-type boundary central charge  $b$  is always positive since it is related to the Zamolodchikov norm of displacement operator, i.e.,  $b = C_D \pi / 32 > 0$ . The displacement operator  $D(y)$  describes the violation of space translation invariance normal to the boundary [21], i.e.,  $\nabla_i T^{ij} = \delta(x) D(y) n^j$ . The two-point function defines its Zamolodchikov norm, i.e.,  $\langle D(y) D(0) \rangle = C_D / |y|^6$ . By definition,  $C_D = 32b/\pi$  is always positive. Thus, we propose the ratio of Casimir amplitude to norm of displacement operator has a lower bound set by holography

$$\left( \frac{-\kappa_1}{C_D} \right) \geq -\frac{\pi^{5/2} \Gamma\left(\frac{1}{3}\right)^3}{108 \Gamma\left(\frac{5}{6}\right)^3} \approx -2.17, \quad \text{for 3d CFTs.} \quad (3)$$

Remarkably, unlike the KSS bound (1), different holographic models give the same universal lower bound (3) for Casimir effect. We verify the lower bound (3) by free CFTs, Ising model, and  $O(N)$  model with  $N = 2, 3$  at critical points. See Table. I. Below we discuss the derivation of the holographic lower bound and its various tests and generalizations. We focus on natural units with  $c = \hbar = k_B = 1$  in the followings.

*Holographic bound* — Let us study the holographic bound of the Casimir effect of a strip in AdS/BCFT [22]. We

TABLE I.  $(-\kappa_1/C_D)$  for various 3d CFTs

Fermion	Scalar	Ising	O(2)	O(3)	Holography
-1.42	-1.89	-2.12	-1.83	-1.62	-2.17

are interested in the general ghost-free gravity in  $\text{AdS}_4$ , which turns out to be Dvali-Gabadadze-Porrati (DGP) gravity [23]  $I = \int_N d^4x \sqrt{|g|} (R+6) + 2 \int_Q d^3y \sqrt{|h|} (K - T + \lambda \mathcal{R})$ , where  $K$  is the extrinsic curvature,  $T$  is the brane tension,  $\lambda$  is the DGP parameter,  $R$  and  $\mathcal{R}$  are Ricci scalars in bulk  $N$  and on the brane  $Q$  respectively. We have set Newton's constant  $16\pi G_N = 1$  and AdS radius  $l = 1$  for simplicity. Note that higher derivative gravity and negative DGP gravity generally suffer the ghost problems [24], while Gauss-Bonnet/Lovelock gravity appears only in dimensions higher than four. Thus, positive DGP gravity with  $\lambda \geq 0$  is the general well-defined gravity theory in  $\text{AdS}_4$ . Following [22], we impose Neumann boundary condition (NBC) on the brane  $Q$

$$K^{ij} - (K - T + \lambda \mathcal{R}) h^{ij} + 2\lambda \mathcal{R}^{ij} = 0, \quad (4)$$

where  $T = 2 \tanh(\rho) - 2\lambda \operatorname{sech}^2(\rho)$  is a useful parameterization [24]. The holographic norm of the displacement operator is given by [24, 25]

$$C_D = \frac{32}{\pi \left( \frac{2\lambda}{2\lambda \sinh(\rho) + \cosh(\rho)} + 2 \tan^{-1} \left( \tanh \left( \frac{\rho}{2} \right) \right) + \frac{\pi}{2} \right)}. \quad (5)$$

$C_D \geq 0$  together with  $\lambda \geq 0$  yields the constraints:  $0 \leq \lambda$  for  $\rho \geq 0$ ;  $0 \leq \lambda \leq -\frac{\coth(\rho)}{2} \geq 1/2$  for  $\rho \leq 0$ . Note that  $\lambda = 1/2$  is a critical DGP parameter. Below, we will show  $\lambda = 1/2$  is a phase-transition point. In the followings, we show only key points. See appendix for detailed derivations.

The vacuum of a strip is dual to AdS soliton in bulk [20]

$$ds^2 = \frac{\frac{dz^2}{h(z)} + h(z) d\theta^2 - dt^2 + dy^2}{z^2}, \quad (6)$$

where  $h(z) = 1 - z^3/z_h^3$ . By using the rescale invariance of AdS, we set  $z_h = 1$  below. The absence of conical singularities fixes the period of angle  $\theta$  in bulk  $\beta = 4\pi/|h'(1)| = 4\pi/3$ . The strip is defined on the AdS boundary  $z = 0$  with  $0 \leq \theta \leq L$ , where  $L \geq 0$  is the strip width. We derive the energy density  $T_{tt} = -1$  from (6) by applying the holographic renormalization [26]. Compared with the Casimir effect (2), we get the holographic Casimir amplitude

$$\kappa_1 = L^3, \quad (7)$$

where  $L$  can be fixed by NBC (4). For negative brane tension  $T \leq 0$ , we have

$$L_I = \int_0^{z_{\max}} \frac{2 \left( \sqrt{h(z_{\max})} - \lambda h(z) \right) dz}{h(z) \sqrt{H(z, z_{\max}) - h(z_{\max})}}, \quad (8)$$

where  $H = \frac{1}{2} h(z) \left( 1 + 2\lambda \sqrt{h(z_{\max})} + X \right)$ ,  $X = \sqrt{1 + 4\lambda^2 h(z) - 4\lambda \sqrt{h(z_{\max})}}$  and  $z_{\max}$  is the turning point obeying  $T = -2\sqrt{h(z_{\max})}$ . The case with  $T > 0$  can be obtained from the complement of the first case  $L_{II} = \beta - L_I (T \rightarrow -T, \lambda \rightarrow -\lambda)$ . This is the typical trick used in [20], based on extrinsic curvature flip signs when crossing the brane. In the viewpoint of NBC (4),  $T, \lambda$  change signs equivalently. Some comments are in order. First, the integrand of (8) cannot take absolute value, which would miss the case of  $T < 0$  with  $\rho > 0$  and cannot produce the correct asymptotical behavior, i.e.  $\theta = -\sinh(\rho)z + O(z^2)$  and  $(\theta - L) = \sinh(\rho)z + O(z^2)$ . Second,  $L_I$  is negative for sufficiently large  $\lambda$ . Thus, there is an upper bound of  $\lambda$ . In fact, the constraint  $L \geq 0$  yields  $\lambda \leq 1$ . Third, the case  $0 \leq \lambda \leq 1/2$  can continuously transform into that of Einstein gravity, while the case  $1/2 < \lambda \leq 1$  cannot. See Fig. 1 for instance. We name them normal and singular phases, respectively. Fourth, the strip width  $L$  decreases with brane tension  $T$  [20] and  $L \geq 0$  sets an upper bound of  $T$  [27]. For  $T \geq 0$ ,  $L$  should be smaller than angle period  $\beta$  to avoid conical singularity. Luckily,  $L \leq \beta$  is satisfied automatically for  $T \geq 0$  [27]. On the other hand, there is no upper bound of  $L$  for  $T < 0$ , since the conical singularity is hidden behind the brane [28]. Thus, it is irrelevant to the bulk dual of strip. As a result, there is no extra constraint on the lower bound of  $T$  and it can take the minimal value  $T = -2$  ( $\rho \rightarrow -\infty$ ) [27, 28].

We can derive the ratio  $(-\kappa_1/C_D)$  from (5,7,8). See Fig. 1 for example. Fig. 1 (up) denotes the normal phase with  $0 \leq \lambda \leq 1/2$ , which shows that the smaller  $\rho$ , the smaller  $(-\kappa_1/C_D)$ . Besides, all curves approach the same lower bound (purple curve) from the above in the limit  $\rho \rightarrow -\infty$  ( $T \rightarrow -2$ ). On the other hand, Fig. 1 (down) labels the singular phase with  $1/2 < \lambda \leq 1$ . It shows that  $(-\kappa_1/C_D)$  with  $\lambda > 1/2$  is always larger than that of Einstein gravity (blue curve). Besides, the minimum of  $(-\kappa_1/C_D)$  increases with  $\lambda$  and approaches zero when  $\lambda \rightarrow 1$ . Since we are interested in the lower bound of  $(-\kappa_1/C_D)$ , we focus on the normal phase below.

Now, we give some analytical discussions. Performing coordinate transformation  $z = z_{\max}y$  and expanding (8) around  $x = \operatorname{sech}^2(\rho) \rightarrow 0$ , we derive perturbatively for normal phase

$$L_I = \frac{2\sqrt{\pi}\Gamma\left(\frac{4}{3}\right)}{\Gamma\left(\frac{5}{6}\right)} \left( \frac{(1-2\lambda)^2}{x} \right)^{\frac{1}{6}} + (1-2\lambda) O\left(\frac{x}{(1-2\lambda)^2}\right)^{\frac{5}{6}} \quad (9)$$

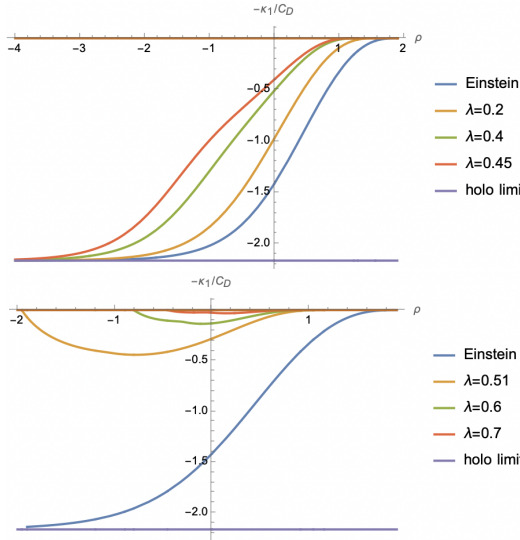


FIG. 1. (up)  $(-\kappa_1/C_D)$  in normal phase with  $0 \leq \lambda \leq 1/2$ ; (down)  $(-\kappa_1/C_D)$  in singular phase with  $1/2 < \lambda \leq 1$ . The left figure shows all curves approach the holographic limit (purple curve) from the above for  $\rho \rightarrow -\infty$  ( $T \rightarrow -2$ ) in the normal phase. The right figure shows  $(-\kappa_1/C_D)$  increases with  $\lambda$  for  $1/2 < \lambda < 1$ . In the limit  $\lambda \rightarrow 1$ , we have  $\kappa_1/C_D \rightarrow 0$  in the singular phase. The two figures imply  $\lambda = 1/2$  is a phase transition point.

Taking limit  $x \rightarrow 0$  ( $T \rightarrow -2$ ) with  $\lambda < 1/2$ , we obtain a universal limit independent of  $\lambda$

$$\lim_{T \rightarrow -2} \left( \frac{-\kappa_1}{C_D} \right) = \lim_{x \rightarrow 0} \left( \frac{-L_I^3}{C_D} \right) = -\frac{\pi^{5/2} \Gamma \left( \frac{1}{3} \right)^3}{108 \Gamma \left( \frac{5}{6} \right)^3}. \quad (10)$$

It verifies our claim that different holographic models give the same lower bound (3) in the normal phase. Note that (9) implies  $L/\beta \rightarrow \infty$  for  $x \rightarrow 0$  ( $T \rightarrow -2$ ). Note also that the strip width  $L \rightarrow Lz_h$  can remain finite when recovering  $z_h \rightarrow 0$  in  $h(z)$  (6). At the phase transition point  $\lambda = 1/2$ , the lower bound (10) can be achieved by  $L = \beta$ . See appendix for derivations. Note that the lower bound of  $(-\kappa_1/C_D)$  is saturated by negative brane tension. We remark that the negative brane tension is well-defined in AdS/BCFT [20, 22, 27, 28]. First, the brane tension is a cosmological constant rather than a kinetic-energy term on the end-of-the-world (EOW) brane. Of course, the negative cosmological constant is well-defined in AdS/CFT. Second, negative brane tension generally yields a negative A-type boundary central charge. But nothing goes wrong. Recall that the free scalar with the DBC has a negative A-type boundary central charge [19].

*Tests* — Let us test the holographic lower bound of the Casimir effect (3) by field theories. First, consider free CFTs. For free Fermions, we have  $(-\kappa_1/C_D) = -3\pi\zeta(3)/8 \approx -1.42$ . For free scalar, we have  $(-\kappa_1/C_D) = -\pi\zeta(3)/2 \approx -1.89$  for both RBC and DBC. Next, for CFTs with interactions. For Ising

model with  $\phi^4$  interaction at the critical point, we have  $2\kappa_1 \approx 0.820$  and  $C_D \approx 0.193$  [29–31], which yields  $(-\kappa_1/C_D) \approx -2.12$ . Near the strip boundary, the scalar operator behaves as [32]

$$\langle \sigma(z) \rangle = \frac{a_\sigma}{(2z)^{\Delta_\sigma}} \left( 1 + B_\sigma \left( \frac{z}{L} \right)^d + \dots \right), \quad (11)$$

where  $\Delta_\sigma$  is the conformal dimension and  $B_\sigma$  obeys the universal relation

$$\frac{B_\sigma}{\Delta_\sigma} = 2^{d-1} (d-1) \pi^{-\frac{d}{2}} \Gamma \left( \frac{d}{2} \right) \frac{\kappa_1}{C_D}. \quad (12)$$

Here, we use the notation of [29] with  $d = 3$  for 3d CFTs. For  $O(N)$  model with  $N = 2, 3$ , [29] obtains  $B_\sigma \approx 1.21, 1.07$  and  $\Delta_\sigma \approx 0.519088, 0.518920$  by applying Monte Carlo simulations. Then (12) gives  $(-\kappa_1/C_D) \approx -1.83, -1.62$  for  $N = 2, 3$ , respectively. We summarize all the above results in Table I, which all obey the holographic bound (3). It strongly supports our proposal. Interestingly, (12) suggests the bound of the Casimir effect imposes an upper bound of  $B_\sigma/\Delta_\sigma$ . Below we briefly comment on various generalizations of our proposal (3). We show only key points and leave detailed discussions and open questions to future work.

*General boundaries* — Holography is expected to set a bound of Casimir effect for general boundary shapes, not be limited to strips. Let us provide some evidence. We first consider the wedge space, which is the simplest generalization of a strip. The Casimir effect takes the form

$$\langle T_j^i \rangle_{\text{wedge}} = \frac{f(\Omega)}{r^3} \text{diag} \left( 1, -2, 1 \right), \quad (13)$$

where  $f(\Omega)$  is the Casimir amplitude and  $\Omega$  is the opening angle of wedge. In the limit  $\Omega \rightarrow 0, r \rightarrow \infty$  with  $r\Omega = L$  fixed, the large  $r$  region of the wedge approaches a strip. It results in  $f(\Omega) \rightarrow \kappa_1/\Omega^3$  for  $\Omega \rightarrow 0$  [33]. On the other hand, we have  $f(\Omega) \rightarrow (C_D\pi/64)(\pi - \Omega)$  in the smooth limit  $\Omega \rightarrow \pi$  [34]. These two limits suggest

$$\left( \frac{-f(\Omega)}{C_D} \right) \geq \left( \frac{-f(\Omega)}{C_D} \right)_{\text{holo}}, \text{ for } 0 < \Omega \leq \pi, \quad (14)$$

where the holographic bound is derived in the limit  $T \rightarrow -2$ . By applying the method of this paper and [34], we numerically verify (14) holds. Let us go on to discuss the general boundary. Near any smooth boundary, the normal-normal component of stress tensor takes a universal form in flat space [33, 35]

$$\langle T_{nn}(z) \rangle = \alpha \frac{\text{Tr} \bar{k}^2}{z} - \frac{\alpha}{2} k \text{Tr} \bar{k}^2 \log \left( \frac{z}{L} \right) + t_{nn} + O(z) \quad (15)$$

where  $k$  and  $\bar{k}$  are the trace and traceless parts of extrinsic curvatures,  $z$  is the distance to boundary,  $L$  is the system size, and  $t_{nn}$  denotes the finite term. The divergent terms appear since we consider the ideal boundary.

There is a natural cutoff  $z \geq \epsilon$  in real material with  $\epsilon$  the lattice length. Remarkably, the displacement operator universally determines the divergent terms, i.e.,  $\alpha = -C_D\pi/16$  [35]. It strongly suggests  $\langle T_{nn}(\epsilon) \rangle/C_D$ , or equivalently,  $t_{nn}/C_D$  has a lower bound for fixed system size and boundary shape. A weaker proposal is for the average pressure

$$\left(\frac{\bar{t}_{nn}}{C_D}\right) \geq \left(\frac{\bar{t}_{nn}}{C_D}\right)_{\text{holo}}, \quad (16)$$

where  $\bar{t}_{nn} = (\int_{\partial M} t_{nn} dS) / (\int_{\partial M} dS)$  is related to the variation of the total energy concerning the system size, i.e.,  $-dE/dL$ .

*Higher dimensions* — Let us comment on the holographic bound of Casimir effect for a strip in higher dimensions. The corresponding Casimir amplitude  $\kappa_1$  and norm of displacement operator  $C_D$  is given by [34] for Einstein gravity. By taking the limit  $\rho \rightarrow -\infty$  ( $T \rightarrow -(d-1)$ ), we derive a universal lower bound

$$\left(\frac{-\kappa_1}{C_D}\right) \geq \frac{-2^{d-2} d \pi^{d-\frac{1}{2}} \Gamma\left(\frac{d-1}{2}\right) \Gamma\left(\frac{1}{d}\right)^d}{\Gamma(d+2) \left(d \Gamma\left(\frac{1}{2} + \frac{1}{d}\right)\right)^d}. \quad (17)$$

We verify that DGP gravity, Gauss-Bonnet/Lovelock gravity yield the same lower bound in the normal phase. We also verify that free scalar obeys the bound, i.e.,  $(-\kappa_1/C_D)_{\text{scalar}} = -2^{1-d} \pi^{d/2} \zeta(d) / \Gamma\left(\frac{d}{2}\right) \geq (17)$ . For  $d > 3$ , there are more boundary central charges. If ratios of  $\kappa_1$  and various boundary central charges have similar bounds is an interesting question. We leave it and more tests of the holographic bound (17) to future works.

*Non-CFTs* — Interestingly, the lower bound of (3) also works for a general class of non-CFTs. Take an example of a 3d free scalar with mass  $m$  and coupling  $\xi$  with the Ricci scalar. It is a CFT only if  $\xi = 1/8$  and  $m = 0$ . For non-CFT parameters, the energy density between parallel plates is no longer a constant [5]. What is worse, it is divergent near the boundary. Fortunately, the total energy per area is finite [5]. On the other hand, the pressure is still a finite constant. Thus, we define  $\kappa_1 = \langle T_{nn}(0) \rangle L^3 / (-2)$  generally. By applying the textbook method, we obtain for both RBC and DBC, i.e.,  $16\pi\kappa_1 = -2M^2 \log(1 - e^{-2M}) + 2M \text{Li}_2(e^{-2M}) + \text{Li}_3(e^{-2M})$ , where  $M = mL > 0$  is a dimensionless parameter, and  $\text{Li}$  denotes the Polylogarithmic function. Remarkably,  $\kappa_1$  is independent of  $\xi$  and decreases with mass

$$\frac{d\kappa_1}{dM} = \frac{M^2(1 - \coth(M))}{8\pi} < 0. \quad (18)$$

It means the Casimir effect is suppressed by mass [5]. For non-CFTs, we can define  $C_D$  via  $\langle D(y)D(0) \rangle = C_D/|y|^6 + O(1/|y|^5)$  in half space, where  $D = T_{nn}(0)$  [21]. At small distance  $m|y| \ll 1$ , the mass effect can be

ignored. As a result,  $C_D$  is independent of mass. The above discussions show  $(-\kappa_1/C_D)$  is larger than that of free scalar, thus obeys the holographic lower bound (3) too. The above arguments apply to general massive free field theories.

*Discussions* — In conclusion, we propose that holography sets a fundamental bound for the ratio of Casimir amplitude and the norm of displacement operator. The Casimir amplitude is generally defined as the average pressure  $\bar{t}_{nn}$  on the boundary. We take 3d CFTs in a strip as an example and then briefly discuss the generalization to other boundary shapes, higher dimensions, and non-CFTs. This paper focuses on flat space and the same boundary conditions on two parallel plates. It is interesting to test our proposal in experiments of critical systems [36]. Finding a field-theoretical proof or counterexample for the holographic bound of the Casimir effect is also enjoyable. Usually, a bound is set by either free or strongly coupled theory. For entanglement entropy (EE), there is a similar bound set by free theory, i.e.,  $(-F_0/C_T) \geq (-F_0/C_T)_{\text{free scalar}}$  [37], where  $F_0$  is the universal coefficient of EE and  $C_T$  is a bulk central charge. We remark that the dual brane for EE is tensionless while the one for the Casimir effect is tensile. With a tensile brane, we have more parameters to get a smaller lower bound of Casimir effect in holography than in free theory. In  $\text{AdS}_3$ , conformal bootstrap restricts brane tension  $|T| \leq 0.99$  slightly stronger than  $|T| \leq 1$  [38]. If this is also the case for both  $T$  and DGP coupling  $\lambda$  in higher dimensions, it may give a slightly stronger lower bound of the Casimir effect. Anyway, this paper gives an important step toward exploring the lower bound of the Casimir effect. Many open problems remain to be explored.

## ACKNOWLEDGEMENTS

We thank T. Takayanagi, J. X. Lu for valuable comments and discussions. We are grateful to the conference “Gauge Gravity Duality 2024”, where the work was completed. This work is supported by the National Natural Science Foundation of China (No.12275366).

## Bound of Casimir effect from DGP gravity

This appendix studies the holographic bound of Casimir effect in DGP gravity. In particular, we give detailed derivations of eqs.(8, 10) in the main text.

Let us quickly recall some key points. The vacuum of a strip is dual to  $\text{AdS}$  soliton

$$ds^2 = \frac{\frac{dz^2}{h(z)} + h(z)d\theta^2 - dt^2 + dy^2}{z^2}, \quad (19)$$

where  $h(z) = 1 - z^3$ , and  $\theta$  has the range  $0 \leq \theta \leq L$  on the AdS boundary  $z = 0$ . We label the embedding function of brane  $Q$  as

$$\theta = S(z). \quad (20)$$

It obeies NBC

$$K^{ij} - (K - T + \lambda\mathcal{R})h^{ij} + 2\lambda\mathcal{R}^{ij} = 0, \quad (21)$$

where the tension is parameterized as [24]

$$T = 2\tanh(\rho) - 2\lambda\operatorname{sech}^2(\rho). \quad (22)$$

This parameterization can be derived from the gravity dual of half space. Since the region near any smooth boundary can be approximately by half space, it works for general boundaries. Substituting (20) into NBC (21), we derive near the two boundaries of strip

$$\theta = -\sinh(\rho)z + O(z^2), \quad \theta - L = \sinh(\rho)z + O(z^2). \quad (23)$$

Let us first study the case with negative brane tension  $T \leq 0$ , the other case with  $T > 0$  can be obtained by the complement of the first case. This is the typical trick used in [20]. Let us explain more. See Fig. 2 for the geometry of holographic dual of strip. The region between red/blue curves (branes) and black line is the bulk dual of strip I with  $T \leq 0$ ; its complement in bulk is the gravity dual for strip II (green line) with  $T > 0$ . As shown in Fig. 2, the gravity duals of strip I and strip II shares the same EOW branes (blue curve or red curve depending on the theory parameters). As a result, the NBCs (21) for strip I and strip II take the same values. However, the extrinsic curvatures  $K_{ij}$  flip signs, while the induced metric  $h_{ij}$  and intrinsic Ricci tensor  $\mathcal{R}_{ij}$  remain invariant when crossing the branes. In the viewpoint of NBC (21),  $T$  and  $\lambda$  change signs when crossing the branes. Note that the bulk dual for strip II contains the ‘horizon’  $z = z_h$ . To remove the conical singularity at  $z = z_h$ , we fix the period of angle  $\theta$  as  $\beta = 4\pi/|h'(z_h)| = 4\pi z_h/3$ . Thus for  $T > 0$ , the left and right vertical dotted lines of Fig. 2 are identified due to the periodicity of angle  $\theta$ . On the other hand, for strip I with  $T \leq 0$ , the ‘horizon’ and potential conical singularity is hidden behind the branes (red/blue curves). Thus, the conical singularity is irrelevant and  $\theta$  can be non-periodic for  $T \leq 0$ .

Without loss of generality, we focus on the strip I with  $T \leq 0$  below. According to (23), the blue and red curves of Fig. 2 correspond to  $\rho < 0$  and  $\rho > 0$ , respectively. We focus on the left half of branes, the right half can be obtained by symmetry. NBC (21) yields an independent equation for  $T \leq 0$

$$T = -\frac{2h(z)\left(h(z)S'(z)\sqrt{h(z)S'(z)^2 + \frac{1}{h(z)}} + \lambda\right)}{h(z)^2S'(z)^2 + 1}. \quad (24)$$

Let us verify that it corresponds to the left half of branes. From (22,24), we derive  $S'(0) = -\sinh(\rho)$  near  $\theta_1$  of Fig.

2, which agrees with the first equation of (23). As shown in Fig. 2, we have  $S'(z_{\max}) = \infty$  and  $S'(z_c) = 0$  at the turning points  $z_{\max}$  and  $z_c$  for the left half of branes. Substituting  $S'(z_{\max}) = \infty$  and  $S'(z_c) = 0$  into (24), we obtain

$$T = -2\sqrt{h(z_{\max})} = -2\lambda h(z_c). \quad (25)$$

Note that there is no turning point  $z_c$  for the blue curve with  $\rho < 0$ . Instead, it appears only in the red curve with  $\rho > 0$ . Solving (24) and (25), we get

$$S'(z) = \pm \frac{\sqrt{h(z_{\max})} - \lambda h(z)}{h(z)\sqrt{H(z, z_{\max}) - h(z_{\max})}}, \quad (26)$$

where  $H = \frac{1}{2}h(z)\left(1 + 2\lambda\sqrt{h(z_{\max})} + X\right)$ ,  $X = \sqrt{1 + 4\lambda^2h(z) - 4\lambda\sqrt{h(z_{\max})}}$ . We choose the positive sign, i.e.,  $S'(z) \sim (\sqrt{h(z_{\max})} - \lambda h(z))$ , for the left halves of red and blue curves to get the correct behavior  $S'(0) = -\sinh(\rho)$  near  $\theta_1$  of Fig. 2. The negative sign of (26) corresponds to the right halves of branes. From (20,26), we derive the width of strip I for  $T \leq 0$

$$L_I = \int_0^{z_{\max}} \frac{2\left(\sqrt{h(z_{\max})} - \lambda h(z)\right) dz}{h(z)\sqrt{H(z, z_{\max}) - h(z_{\max})}}, \quad (27)$$

where  $z_{\max} = (1 - T^2/4)^{1/3}$  from (25). We stress that the above formula works for both the cases of blue curve and red curve of Fig. 2. In particular, the integrand  $2S'(z) \sim 2(\sqrt{h(z_{\max})} - \lambda h(z))$  flips signs at turning point  $z_c$  (25), which is the expected feature for the red curve. It suggests the integrand cannnot be chosen as the absolute value  $2|S'(z)| \sim 2|\sqrt{h(z_{\max})} - \lambda h(z)|$ , which would miss the case of red curve.

Recall that strip II is the complement of strip I and  $(T, \lambda)$  of NBC (4) flip signs when crossing the brane, we get the width of strip II for  $T \geq 0$

$$L_{II} = \beta - L_I(T \rightarrow -T, \lambda \rightarrow -\lambda), \quad (28)$$

where, as we discuss above, the angle period  $\beta = 4\pi z_h/3$  is meaningful only for  $T \geq 0$ . In total, we have

$$L = \begin{cases} L_I, & \text{for } T \leq 0, \\ L_{II}, & \text{for } T \geq 0. \end{cases} \quad (29)$$

One can check  $L$  is continuous at  $T = 0$ , which is a test of our results. See Fig. 3 for example. As mentioned in main text, the constraint  $0 \leq L$  set an upper bound of  $\lambda$ . It is clear from (27) that too large  $\lambda$  would give negative  $L$ . We numerically find the range  $0 \leq \lambda \leq 1$ . We name the range  $0 \leq \lambda < 1/2$  the ‘norm phase’, since the strip width  $L$  can continuously transform into that of Einstein

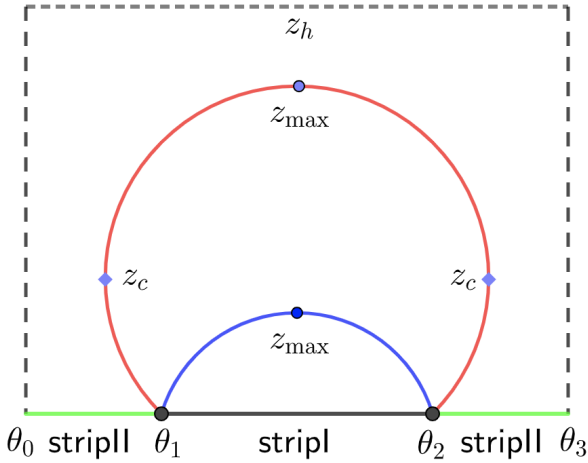


FIG. 2. Geometry of holographic strip: a portion of AdS soliton. The region between red/blue curves (branes) and black line is the bulk dual of strip I with negative brane tension  $T \leq 0$ ; its complement in bulk is the gravity dual for strip II (green line) with  $T > 0$ . The gravity dual of strip II contains the ‘horizon’  $z = z_h$ . To remove the conical singularity on it, the angle  $\theta$  should be periodic. Thus green lines for strip II are connected. Without loss of generality, we focus on strip I with  $T \leq 0$ . We have ( $\rho < 0$ ) and ( $\rho > 0$ ) for the blue and red curves, respectively.  $z_{\max}$  and  $z_c$  denote the turning points with  $\theta'(z_{\max}) = \infty$  and  $\theta'(z_c) = 0$ .

gravity. See Fig. 3 (left). On the other hand, we call the range  $1/2 \leq \lambda \leq 1$  the ‘singular phase’, because it cannot continuously transform into that of Einstein gravity. See Fig. 3 (right).  $\lambda = 1/2$  is the phase-transition point.

Now we make some analytical discussions. Performing coordinate transformation  $z = z_{\max}y$  and expanding (8) around  $x = \operatorname{sech}^2(\rho) \rightarrow 0$ , we derive perturbatively for normal phase

$$\begin{aligned} L_I &= \int_0^1 dy \frac{2\sqrt[3]{1-2\lambda}}{\sqrt[6]{x}\sqrt{1-y^3}} + (1-2\lambda) O\left(\frac{x}{(1-2\lambda)^2}\right)^{\frac{5}{6}} \\ &= \frac{2\sqrt{\pi}\Gamma\left(\frac{4}{3}\right)}{\Gamma\left(\frac{5}{6}\right)} \left(\frac{(1-2\lambda)^2}{x}\right)^{\frac{1}{6}} + (1-2\lambda) O\left(\frac{x}{(1-2\lambda)^2}\right)^{\frac{5}{6}} \end{aligned} \quad (30)$$

The norm of displacement operator becomes for  $\rho < 0$

$$C_D = \frac{32}{\frac{2\pi\lambda\sqrt{x}}{1-2\lambda\sqrt{1-x}} + \pi \cot^{-1}\left(\sqrt{\frac{1}{x}-1}\right)}. \quad (31)$$

Taking the limit  $x \rightarrow 0$  ( $\rho \rightarrow -\infty$ ) with  $\lambda < 1/2$ , we obtain a universal limit

$$\lim_{\rho \rightarrow -\infty} -\frac{\kappa_1}{C_D} = \lim_{x \rightarrow 0} -\frac{L_I^3}{C_D} = -\frac{\pi^{5/2}\Gamma\left(\frac{1}{3}\right)^3}{108\Gamma\left(\frac{5}{6}\right)^3}, \quad (32)$$

in normal phase with  $0 \leq \lambda < 1/2$ . Note that  $L_I$  (30) goes to infinity for  $x \rightarrow 0$  ( $\rho \rightarrow -\infty$ ). Recovering  $z_h$  in

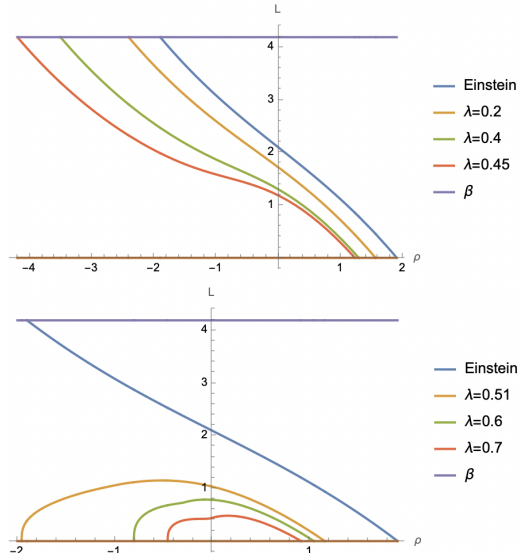


FIG. 3. (Left) strip widths in normal phase with  $0 \leq \lambda \leq 1/2$ ; (Right) (Left) strip widths in singular phase with  $1/2 \leq \lambda \leq 1$ . Note that  $L$  can be larger than  $\beta$  for negative enough  $\rho$  in the normal phase. We show only range of  $L \leq \beta$  for simplicity. On the other hand,  $L$  is always smaller than  $\beta$  in the singular phase. In both cases, the condition  $0 \leq L$  imposes an upper bound of  $\rho$ .

$h(z) = 1 - z^3/z_h^3$ , we can keep the strip width  $L \rightarrow z_h L$  finite in the limit  $\rho \rightarrow -\infty$  and  $z_h \rightarrow 0$ . Let us go on to discuss the case at the phase transition point  $\lambda \rightarrow 1/2$ . For our purpose, we consider the limit  $x \rightarrow 0$ ,  $\lambda \rightarrow 1/2$  with  $x/(1-2\lambda)^2$  finite. In such limit, (30) becomes

$$L_I \rightarrow \frac{2\sqrt{\pi}\Gamma\left(\frac{4}{3}\right)}{\Gamma\left(\frac{5}{6}\right)} \left(\frac{(1-2\lambda)^2}{x}\right)^{\frac{1}{6}}. \quad (33)$$

Interestingly, the second term of (9) vanishes for  $\lambda \rightarrow 1/2$ . In fact, one can check that this is also the case for higher-order expansions of (9). From (33) and  $L_I = \beta = 4\pi/3$ , we solve

$$x = \frac{729\Gamma\left(\frac{4}{3}\right)^6}{64\pi^3\Gamma\left(\frac{5}{6}\right)^6} (1-2\lambda)^2 + O(1-2\lambda)^3, \quad (34)$$

which implies  $x \rightarrow 0$  ( $\rho \rightarrow -\infty$ ) as  $\lambda \rightarrow 1/2$ . Substituting (34) into (31), we get

$$C_D = \frac{256\sqrt{\pi}\Gamma\left(\frac{5}{6}\right)^3}{27\Gamma\left(\frac{4}{3}\right)^3} + O(\lambda - \frac{1}{2}). \quad (35)$$

Finally, we obtain

$$\lim_{\lambda \rightarrow 1/2, L=\beta} \left(-\frac{\kappa_1}{C_D}\right) = \lim_{\lambda \rightarrow 1/2} \left(-\frac{\beta^3}{C_D}\right) = -\frac{\pi^{5/2}\Gamma\left(\frac{1}{3}\right)^3}{108\Gamma\left(\frac{5}{6}\right)^3}, \quad (36)$$

which reproduces the universal limit (10). Interestingly,  $L = \beta$  instead of  $L/\beta \rightarrow \infty$  at the phase transition point  $\lambda \rightarrow 1/2$ .

---

[1] H. B. G. Casimir, *Indag. Math.* **10**, no.4, 261-263 (1948)

[2] G. Plunien, B. Muller and W. Greiner, *Phys. Rept.* **134**, 87-193 (1986)

[3] M. Bordag, U. Mohideen and V. M. Mostepanenko, *Phys. Rept.* **353**, 1-205 (2001)

[4] K. A. Milton, *J. Phys. A* **37**, R209 (2004)

[5] M. Bordag, G. L. Klimchitskaya, U. Mohideen and V. M. Mostepanenko, *Int. Ser. Monogr. Phys.* **145**, 1-768 (2009) Oxford University Press, 2009

[6] S. Wang, Y. Wang and M. Li, *Phys. Rept.* **696**, 1-57 (2017)

[7] L. Vepstas, A. D. Jackson and A. S. Goldhaber, *Phys. Lett. B* **140**, 280-284 (1984)

[8] M. S. Morris, K. S. Thorne and U. Yurtsever, *Phys. Rev. Lett.* **61**, 1446-1449 (1988)

[9] J. Maldacena and A. Milekhin, *Phys. Rev. D* **103**, no.6, 066007 (2021)

[10] U. Mohideen and A. Roy, *Phys. Rev. Lett.* **81**, 4549-4552 (1998)

[11] G. Bressi, G. Carugno, R. Onofrio and G. Ruoso, *Phys. Rev. Lett.* **88**, 041804 (2002)

[12] G. L. Klimchitskaya, U. Mohideen and V. M. Mostepanenko, *Rev. Mod. Phys.* **81**, 1827-1885 (2009)

[13] J. M. Maldacena, *Int. J. Theor. Phys.* **38**, 1113 (1999) [*Adv. Theor. Math. Phys.* **2**, 231 (1998)] [[hep-th/9711200](#)].

[14] P. Kovtun, D. T. Son and A. O. Starinets, *Phys. Rev. Lett.* **94**, 111601 (2005)

[15] G. Policastro, D. T. Son and A. O. Starinets, *Phys. Rev. Lett.* **87**, 081601 (2001)

[16] M. Brigante, H. Liu, R. C. Myers, S. Shenker and S. Yaida, *Phys. Rev. D* **77**, 126006 (2008)

[17] Y. Kats and P. Petrov, *JHEP* **01**, 044 (2009)

[18] M. Brigante, H. Liu, R. C. Myers, S. Shenker and S. Yaida, *Phys. Rev. Lett.* **100**, 191601 (2008)

[19] K. Jensen and A. O'Bannon, *Phys. Rev. Lett.* **116**, no.9, 091601 (2016)

[20] M. Fujita, T. Takayanagi and E. Tonni, *JHEP* **11**, 043 (2011)

[21] M. Billò, V. Gonccalves, E. Lauria and M. Meineri, *JHEP* **04**, 091 (2016)

[22] T. Takayanagi, *Phys. Rev. Lett.* **107** (2011) 101602 [[arXiv:1105.5165 \[hep-th\]](#)].

[23] G. R. Dvali, G. Gabadadze and M. Porrati, *Phys. Lett. B* **485**, 208-214 (2000)

[24] R. X. Miao, *JHEP* **06**, 043 (2024)

[25] R. X. Miao, *JHEP* **07**, 098 (2019)

[26] S. de Haro, S. N. Solodukhin and K. Skenderis, *Commun. Math. Phys.* **217**, 595-622 (2001)

[27] M. Miyaji, T. Takayanagi and T. Ugajin, *JHEP* **06**, 023 (2021)

[28] We thank Takayanagi for valuable comments on negative brane tension and its irrelevance to conical singularity.

[29] F. P. Toldin and M. A. Metlitski, *Phys. Rev. Lett.* **128**, no.21, 215701 (2022)

[30] F. Parisen Toldin, S. Dietrich, *J.Stat.Mech.* 2010 P11003

[31] M. Hasenbusch, *Phys.Rev.B* 82 (2010) 104425

[32] J. L. Cardy, *Phys. Rev. Lett.* **65**, 1443-1445 (1990)

[33] D. Deutsch and P. Candelas, *Phys. Rev. D* **20**, 3063 (1979)

[34] R. X. Miao, *JHEP* **06**, 084 (2024)

[35] R. X. Miao and C. S. Chu, *JHEP* **1803**, 046 (2018)

[36] M. Krech, *The Casimir Effect in Critical Systems* (World Scientific, London, 1994).

[37] P. Bueno, H. Casini, O. L. Andino and J. Moreno, *Phys. Rev. Lett.* **131**, no.17, 171601 (2023)

[38] S. Collier, D. Mazac and Y. Wang, *JHEP* **02**, 019 (2023)